Bright spatial solitons in defocusing Kerr media with $\mathcal{PT}$-symmetric potentials

Zhiwei Shi,[1] Xiujuan Jiang,[1] Xing Zhu,[2] and Huagang Li[3,*]

[1]*School of Information Engineering, Guangdong University of Technology, Guangzhou 510006, China*

[2]*State Key Laboratory of Optoelectronic Materials and Technologies, Sun Yat-Sen University, Guangzhou 510275, P.R. China*

[3]*Department of Physics, Guangdong Institute of Education, Guangzhou 510303, China*

(Received 1 September 2011; published 28 November 2011)

We show that defocusing Kerr media with parity-time-symmetric potentials can support one- and two-dimensional bright spatial solitons. These solitons are found to be stable over the wide range where they exist. More importantly, we discover an exact one-dimensional solution and a closed two-dimensional solution in the structure.

DOI: 10.1103/PhysRevA.84.053855 PACS number(s): 42.65.Tg, 42.65.Jx, 42.65.Wi

I. INTRODUCTION

It is well known that bright spatial solitons can only exist for focusing nonlinearity in the planar waveguide [1]. Defocusing Kerr nonlinearity usually induces an enhanced beam broadening so that it does not support any localized structure other than vortices and dark solitons, which require a background beam [1,2]. However, the bright solitons can exist in periodic photonic lattices or waveguide arrays with defocusing nonlinearity [3–5]. This means that transverse periodic refractive index potentials can be strong enough not only to suppress the beam broadening that is due to diffraction, but also to overcome the broadening effect of the defocusing Kerr nonlinearity [1].

Recently, parity-time ($\mathcal{PT}$)-symmetric potentials were introduced into optical field [6–17]. The definitions of $\mathcal{PT}$ potentials and their properties have been discussed in the past few years [18–22]. The real part of $\mathcal{PT}$-symmetric potentials must be a symmetric function of position, while the imaginary component should be antisymmetric. In optics, such complex $\mathcal{PT}$-symmetric structures can be designed by introducing a complex refractive-index distribution $n(x) = n_R(x) + in_I(x)$ into the wave-guided system, where $n_R(x) = n_R(-x), n_I(x) = -n_I(-x)$, and x is the normalized transverse coordinate [6,9,10,15]. In the nonlinear domain, a novel class of nonlinear self-trapped modes was found, and the interplay between the Kerr nonlinearity and the $\mathcal{PT}$ threshold was analyzed for the first time [6]. The analytical periodic solutions to a class of nonlinear Schrödinger equations with $\mathcal{PT}$-like potentials [7] and the stable dissipative defect modes in both focusing and defocusing media with strong two-photon absorption [8] were also stated. We also numerically study the existence and stability of gap solitons in $\mathcal{PT}$ complex periodic optical lattices with the real part of superlattices and the gray solitons in $\mathcal{PT}$-symmetric potentials [23,24]. However, thus far all studies have focused on bright solitons in self-focusing optical $\mathcal{PT}$-symmetric media, and bright spatial solitons in Kerr self-defocusing media with a single $\mathcal{PT}$ complex potential are never reported.

In this paper, we investigate a class of one- and two-dimensional stable bright spatial solitons in Kerr self-defocusing media with $\mathcal{PT}$-symmetric potentials. We show that the existing and stable ranges of these solitons are the same. Importantly, an exact one-dimensional solution and a closed two-dimensional solution are found. This indicates that the single $\mathcal{PT}$ complex potential can be strong enough to suppress the beam broadening caused by diffraction and defocusing Kerr nonlinearity.

II. ANALYTICAL AND NUMERICAL SOLITON SOLUTIONS

In a Kerr self-defocusing medium with $\mathcal{PT}$-symmetric potentials, the one-dimensional optical beam evolution is governed by the following normalized nonlinear Schrödinger-like equation for the dimensionless light field amplitude q [6–17],

$$i\frac{\partial q}{\partial z} + \frac{\partial^2 q}{\partial x^2} + Rq - |q|^2 q = 0, \tag{1}$$

where z is the propagation distance, $R = V(x) + iW(x)$, and $V(x)$ and $W(x)$ are the real and imaginary components of the complex $\mathcal{PT}$-symmetric potential, respectively. $V(x)$ is an even function and $W(x)$ is odd. Physically, $V(x)$ is associated with index guiding while $W(x)$ represents the gain or loss distribution of the optical potential. We are going to search for a stationary soliton solution of Eq. (1) in the form of $q(x,z) = u(x)e^{ibz}$, where u is a complex function and b is the propagation constant of spatial solitons. In this case, u satisfies

$$\frac{\partial^2 u}{\partial x^2} + [V(x) + iW(x)]u - |u|^2 u - bu = 0. \tag{2}$$

Here, we assume a Scarff II potential shown in Fig. 1(a) where $V(x) = V_0\mathrm{sech}^2(x)$ and $W(x) = W_0\mathrm{sech}(x)\tanh(x)$, with V_0 and W_0 being the amplitudes of the real and imaginary parts [6,7,21]. Although the $\mathcal{PT}$-symmetric potential has crossed the phase transition point, the solitons still exist because the amplitude of the refractive-index distribution can be altered by the beam itself through the optical nonlinearity. The $\mathcal{PT}$ symmetric will remain broken if it cannot be nonlinearly restored [6,7,9,10].

Equation (2) admits an exact solution of the form $u(x) = u_0\mathrm{sech}(x)\exp\{i\rho\tan^{-1}[\sinh(x)]\}$, where $\rho = W_0/3$, $b = 1$, and $u_0 = \sqrt{V0 - (w_0^2/9) - 2}$. In order to validate the exact solution, we numerically solve Eq. (2) using the spectral renormalization method [25]. As is shown in Fig. 1(b), the

*lihuagang@gdei.edu.cn

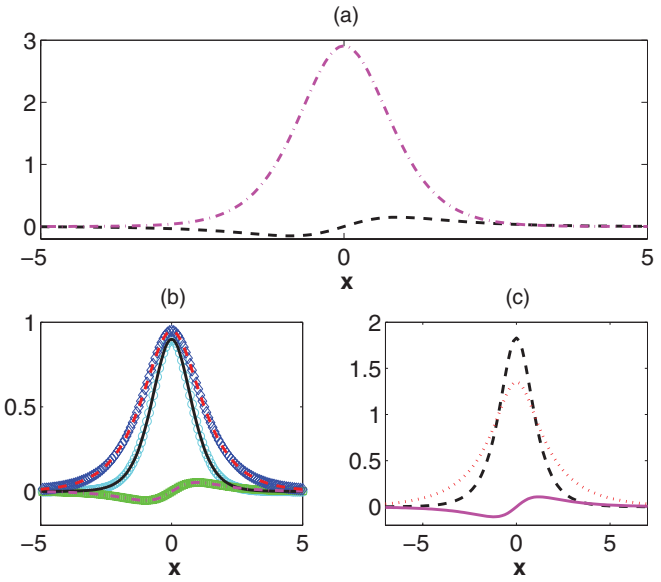

FIG. 1. (Color online) (a) The real (dashed black curve) and imaginary (dash-dotted pink curve) of the Scarff II potential at $b = 1$. (b) $|u(x)|^2$ (cyan circle curve), the real (blue diamond curve) and imaginary components (green square curve) of the exact solution and $|u(x)|^2$ (solid black curve), the real (dashed red curve) and imaginary components (dash-dotted pink curve) of the numerical solution at $b = 1$. (c) The real (dotted red curve), imaginary components (dash-dotted pink curve), and $|u(x)|^2$ (dashed black curve) of the bright soliton gained numerically at $b = 0.31$. The potential parameters are $V_0 = 2.91$ and $W_0 = 0.3$ in (a), (b), and (c).

intensity $|u(x)|^2$, the real and imaginary components of the numerical and exact solutions, are coincident. The other nonlinear mode of the potential with $V_0 = 2.91$ and $W_0 = 0.3$ at $b = 0.31$ is depicted in Fig. 1(c). Evidently, the change of b can influence the solutions.

For all types of solutions, the power $P = \int_{-\infty}^{\infty} |u(x)|^2 dx$ is a monotonically decreasing function of b at $V_0 = 2.91$ and $W_0 = 0.3$ [Fig. 2(a)]. Evidently, the existing range of the solitons is from the lower cutoff b_{low} ($\approx$0.31) to the upper cutoff b_{upp} ($\approx$1.63). To check the stability of the solitons with the method of linear stability analysis, we assume $q(x) = u(x)e^{ibz} + \epsilon[F(x)e^{i\delta z} + G^*(x)e^{-i\delta^* z}]e^{ibz}$, where $\epsilon \ll 1$, F and G are the perturbation eigenfunctions, and δ is the growth rate of the perturbation. By linearizing Eq. (1), we gain [6]

$$\delta F = \left(\frac{\partial^2}{\partial x^2} + V(x) + iW(x) - 2|u|^2 - b\right)F + u^2 G, \quad (3)$$

$$\delta G = \left(-\frac{\partial^2}{\partial x^2} - V(x) + iW(x) + 2|u|^2 + b\right)G - u^{*2}F. \quad (4)$$

The bright spatial soltions are linearly unstable when δ has an imaginary component. On the contrary, they are stable when δ is real. In Fig. 2(a), Im(δ), the imaginary component of δ, is zero, so the solitons are always stable. Importantly, the stability range of solitons is coincident with their existing range. To examine linear stability results, we simulate the stable propagation of beams with the initial input $q|_{z=0} = u(1 + \rho_1)$ under different conditions, as is presented in Figs. 2(b)– 2(d), where ρ_1 is a broadband random perturbation.

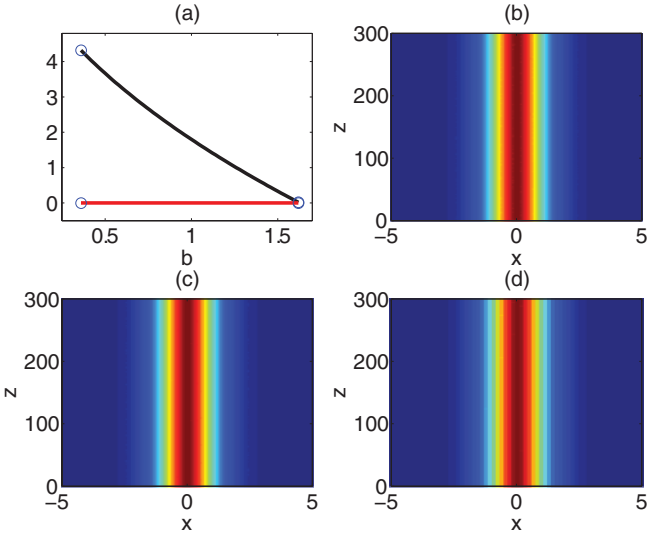

FIG. 2. (Color online) (a) P (black, upper curve) and Im(δ) (red, lower curve) and vs b at $V_0 = 2.91$ and $W_0 = 0.3$. Point marked with circle corresponds to the b_{low} and b_{upp}, respectively. (b) and (c) Simulated propagation of the numerical and exact solitons in Fig. 1(b), with 3% random noise. (d) Simulated propagation of the soliton in Fig. 1(c), with 3% random noise.

Finally, we discuss the formation of $\mathcal{PT}$ bright spatial solitons in two-dimensional symmetric geometries. In this case, Eq. (1) takes the form

$$i\frac{\partial q}{\partial z} + \nabla_\perp^2 q + Rq - |q|^2 q = 0, \quad (5)$$

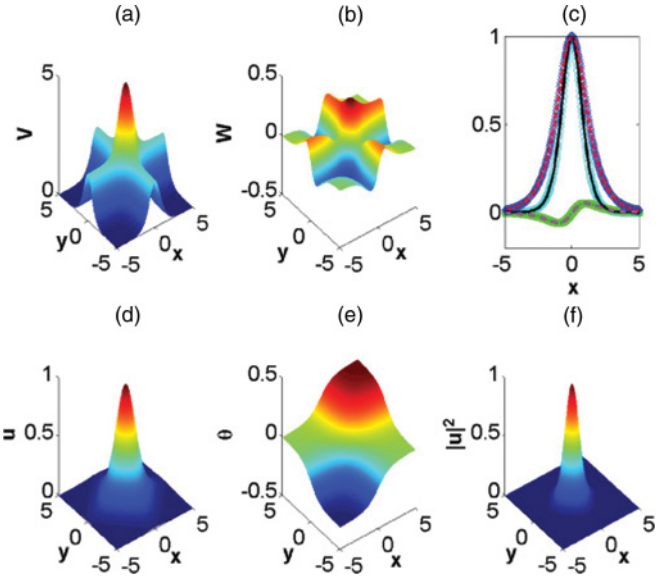

FIG. 3. (Color online) (a) The real and (b) the imaginary of the two-dimensional complex potential. (c) $|u(x,0)|^2$ (cyan circle curve), the real (blue diamond curve) and imaginary components (green square curve) of the exact solution and $|u(x,0)|^2$ (solid black curve), the real (dashed red curve) and imaginary components (dash-dotted pink curve) of the numerical solution in $y = 0$ plane. (d) The eigenfunction $u(x,y)$, (e) the phase θ, and (f) the intensity $|u(x,y)|^2$ of the soliton. Parameters are $b = 2$, $V_0 = 3.01$, and $W_0 = 0.3$.

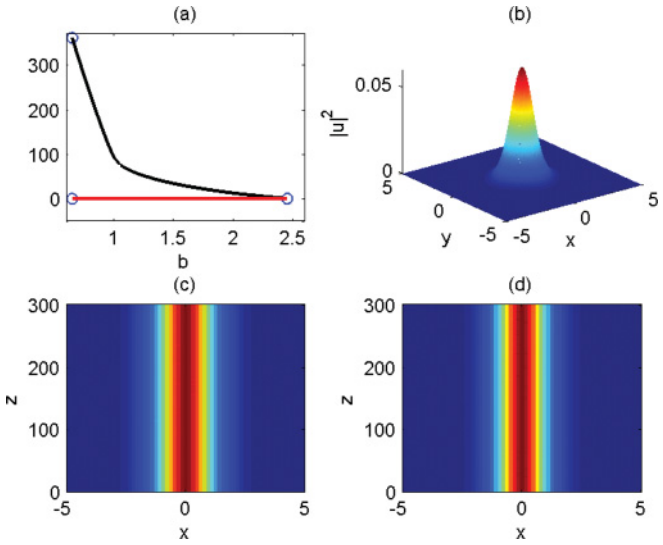

FIG. 4. (Color online) (a) P (black, upper curve) and Im(δ) (red, lower curve) and vs b at $V_0 = 3.01$ and $W_0 = 0.3$. The points marked with circles correspond to b_{low} and b_{upp}, respectively. (b) $|u(x,y)|^2$ of the soliton at $b = 2.45$, $V_0 = 3.01$, and $W_0 = 0.3$. (c) and (d) Simulated propagation of the solitons with 1% random noise corresponding to Fig. 3(f) and Fig. 4(b), respectively.

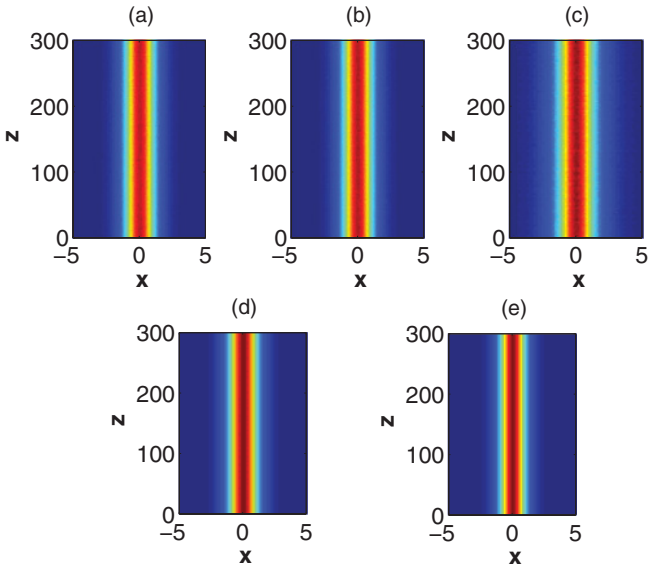

FIG. 5. (Color online) (a)–(e) Simulated propagation of the solitons corresponding to Fig. 1(b), Fig. 1(c), Fig. 3(f), and Fig. 4(b), respectively. In all cases 3% random noise was added to the input field and potential distributions.

where $\nabla_\perp^2 = \partial^2/\partial x^2 + \partial^2/\partial y^2$, $R = V(x,y) + iW(x,y)$, and again the potentials V and W obey the PT-symmetric requirement, $V(-x,-y) = V(x,y)$ and $W(-x,-y) = -W(x,y)$. Figures 3(a) and 3(b), respectively, show the potentials $V(x,y) = (2 + W_0^2/9)[\text{sech}^2(x) + \text{sech}^2(y)] + (V_0^2 - 2 - W_0^2/9)\text{sech}^2(x)\text{sech}^2(y)$ and $W(x,y) = W_0[\tanh(x)\text{sech}(x) + \tanh(y)\text{sech}(y)]$ [7] with $V_0 = 3.01$ and $W_0 = 0.3$. Then, a bound state nonlinear solution to Eq. (5) that satisfies the condition $u \to 0$ as $(x,y) \to \pm\infty$ is sought in the form $q(x,y,z) = u(x,y)\exp[ibz + i\theta(x,y)]$, where $u(x,y) = \sqrt{V_0^2 - 2 - (W_0^2/9)}\,\text{sech}(x)\,\text{sech}(y)$ and $\theta(x,y) = (W_0/3)\{\arctan[\sinh(x)] + \arctan[\sinh(y)]\}$ with the propagation constant $b = 2$. To validate the closed-form solutions, we also numerically solve Eq. (5) with $q(x,y,z) = u(x,y)\exp(ibz)$ using the spectral renormalization method. As is shown in Fig. 3(c), the intensity $|u(x,0)|^2$, the real and imaginary components of the numerical and exact solutions in $y = 0$ plane are coincident. In Figs. 3(d), 3(e) and 3(f), we depict a typical profile of the eigenfunction u, the phase θ, and the intensity $|u|^2$ for $V_0 = 3.01$ and $W_0 = 0.3$, respectively.

The power $P = \int_{-\infty}^{\infty}\int_{-\infty}^{\infty}|u(x,y)|^2 dxdy$ is a monotonically decreasing function of b at $V_0 = 3.01$ and $W_0 = 0.3$. To check the stability of the solitons, we also make the linear stability analysis and show that Im(δ) = 0, and thus the solitons are always stable. Similarly, the stability range of the solitons is the same as their existing range, which is from the lower cutoff b_{low} ($\approx$0.65) to the upper cutoff b_{upp} ($\approx$2.45) [Fig. 4(a)]. To support the linear stability results, we simulate the stable propagation of beams with the initial input $q|_{z=0} = u(1 + \rho_1)$ under different conditions, as is presented in Figs. 4(c) and 4(d).

It is important that the potential is perturbed from a practical viewpoint, so we do the direct numerical simulations of Eqs. (1) and (5) with input conditions $q|_{z=0} = u(1 + \rho_1)$ and $R = R(1 + \rho_2)$, where ρ_2 is also a broadband random perturbation. The results shown in Fig. 5 confirm the stability of solitons.

III. CONCLUSIONS

In conclusion, we investigate a novel class of one- and two-dimensional stable bright spatial solitons in Kerr self-defocusing media with $\mathcal{PT}$-symmetric potentials. These solitons are shown to be stable over a wide range which is the same as their existing range. Importantly, we discover an exact one-dimensional solution and a closed two-dimensional solution in the structure.

[1] O. Bang, Yu. S. Kivshar, and A. V. Buryak, Opt. Lett. **22**, 1680 (1992).
[2] Yu. S. Kivshar, Phys. Rep. **298**, 81 (1998).
[3] Y. Kominis and K. Hizanidis, Opt. Lett. **31**, 2888 (2006).
[4] A. A. Sukhorukov, Phys. Rev. E **65**, 036609 (2002).
[5] Yu. S. Kivshar, Opt. Lett. **18**, 1147 (1993).
[6] Z. H. Musslimani, K. G. Makris, R. El-Ganainy, and D. N. Christodoulides, Phys. Rev. Lett. **100**, 030402 (2008).
[7] Z. H. Musslimani, K. G. Makris, R. El-Ganainy and D. N. Christodoulides, J. Phys. A **41**, 244019 (2008).
[8] Y. V. Kartashov, V. V. Konotop, V. A. Vysloukh, and L. Torner, Opt. Lett. **35**, 1638 (2010).

[9] K. G. Makris, R. El-Ganainy, D. N. Christodoulides, and Z. H. Musslimani, Phys. Rev. Lett. **100**, 103904 (2008).
[10] C. E. Ruter, K. G. Makris, R. El-Ganainy, D. N. Christodoulides, M. Segev, and D. Kip, Nat. Phys. **6**, 192 (2010).
[11] A. Guo, G. J. Salamo, D. Duchesne, R. Morandotti, M. Volatier-Ravat, V. Aimez, G. A. Siviloglou, and D. N. Christodoulides, Phys. Rev. Lett. **103**, 093902 (2009).
[12] S. Longhi, Phys. Rev. Lett. **103**, 123601 (2009).
[13] R. El-Ganainy, K. G. Makris, D. N. Christodoulides, and Z. H. Musslimani, Opt. Lett. **32**, 2632 (2007).
[14] K. G. Makris, R. El-Ganainy, D. N. Christodoulides, and Z. H. Musslimani, Phys. Rev. A **81**, 063807 (2010).
[15] H. Wang and J. D. Wang, Opt. Express **19**, 4030 (2011).
[16] M. V. Berry, J. Phys. A **41**, 244007 (2008).
[17] K. G. Makris, R. El Ganainy, D. N. Christodoulides, and Ziad H. Musslimani, Int. J. Theor. Phys. **50**, 1019 (2011).
[18] C. M. Bender and S. Boettcher, Phys. Rev. Lett. **80**, 5243 (1998).
[19] C. M. Bender, D. C. Brody, and H. F. Jones, Phys. Rev. Lett. **89**, 270401 (2002).
[20] C. M. Bender, D. C. Brody, and H. F. Jones, Am. J. Phys. **71**, 1095 (2003).
[21] Z. Ahmed, Phys. Lett. A **282**, 343 (2001).
[22] C. M. Bender, D. C. Brody, H. F. Jones, and B. K. Meister, Phys. Rev. Lett. **98**, 040403 (2007).
[23] X. Zhu, H. Wang, L. X. Zheng, H. G. Li, and Y. J. He, Opt. Lett. **36**, 2680 (2011).
[24] H. G. Li, Z. W. Shi, X. J. Jiang, and X. Zhu, Opt. Lett. **36**, 3290 (2011).
[25] M. J. Ablowitz and Z. H. Musslimani, Opt. Lett. **30**, 2140 (2005).